

# Secure Cell-Free Integrated Sensing and Communication in the Presence of Information and Sensing Eavesdroppers

Zixiang Ren, *Graduate Student Member, IEEE*, Jie Xu, *Senior Member, IEEE*, Ling Qiu, *Member, IEEE*, and Derrick Wing Kwan Ng, *Fellow, IEEE*

**Abstract**—This paper studies a secure cell-free integrated sensing and communication (ISAC) system, in which multiple ISAC transmitters collaboratively send confidential information to multiple communication users (CUs) and concurrently conduct target detection. Different from prior works investigating communication security against potential information eavesdropping, we consider the security of both communication and sensing in the presence of information and sensing eavesdroppers that aim to intercept confidential communication information and extract target information, respectively. Towards this end, we optimize the joint information and sensing transmit beamforming at these ISAC transmitters for secure cell-free ISAC. Our objective is to maximize the detection probability over a designated sensing area while ensuring the minimum signal-to-interference-plus-noise-ratio (SINR) requirements at CUs. Our formulation also takes into account the maximum tolerable signal-to-noise ratio (SNR) constraints at information eavesdroppers for ensuring the confidentiality of information transmission, and the maximum detection probability constraints at sensing eavesdroppers for preserving sensing privacy. The formulated secure joint transmit beamforming problem is highly non-convex due to the intricate interplay between the detection probabilities, beamforming vectors, and SINR constraints. Fortunately, through strategic manipulation and via applying the semidefinite relaxation (SDR) technique, we successfully obtain the globally optimal solution to the design problem by rigorously verifying the tightness of SDR. Furthermore, we present two alternative joint beamforming designs based on the sensing SNR maximization over the specific sensing area and the coordinated beamforming, respectively. Numerical results reveal the benefits of our proposed design over these alternative benchmarks.

**Index Terms**—Secure integrated sensing and communication (ISAC), information eavesdropping, sensing eavesdropping, joint beamforming design, optimization.

## I. INTRODUCTION

Integrated sensing and communication (ISAC) has been identified as one of the six delineated usage scenarios for

Z. Ren is with the Key Laboratory of Wireless-Optical Communications, Chinese Academy of Sciences, School of Information Science and Technology, University of Science and Technology of China, Hefei 230027, China, and the Future Network of Intelligence Institute (FNii), The Chinese University of Hong Kong (Shenzhen), Shenzhen 518172, China (e-mail: rzx66@mail.ustc.edu.cn).

L. Qiu is with the Key Laboratory of Wireless-Optical Communications, Chinese Academy of Sciences, School of Information Science and Technology, University of Science and Technology of China, Hefei 230027, China (e-mail: lqiu@ustc.edu.cn).

J. Xu is with the School of Science and Engineering (SSE) and the FNii, The Chinese University of Hong Kong (Shenzhen), Shenzhen 518172, China (e-mail: xujie@cuhk.edu.cn).

D. W. K. Ng is with the University of New South Wales, Sydney, NSW 2052, Australia (e-mail: w.k.ng@unsw.edu.au).

L. Qiu and J. Xu are the corresponding authors.

future sixth-generation (6G) wireless networks [1], which holds the capability to support a variety of new applications, such as navigation, activity recognition, environment monitoring, and sensing data acquisition [2], [3]. As a result, ISAC has recently emerged as one of the hottest topics within the wireless communication community, spurring extensive research and development [4]–[6]. The exploration of ISAC for enhancing both sensing and communication performances spans different technical perspectives, including fundamental information theoretic limits [7]–[9], transmit waveform design [10], beamforming optimization [11], [12], active sensing [13], and network architectures [14]. In recent years, the advancements in the multi-antenna technology have significantly enhanced ISAC performance. In particular, the deployment of multiple antennas at ISAC transmitters not only provides multiplexing and diversity gains for substantially enhancing the communication rate and reliability, but also offers additional degrees of freedom (DoFs) for refining sensing resolution and accuracy. Furthermore, besides reusing information beams for the dual sensing purpose, dedicated sensing beams can be additionally exploited to provide full available sensing DoFs. As such, the joint information and sensing beamforming design has emerged as a promising ISAC solution [12], [15]–[17].

While initial ISAC research focused on the single-cell scenarios with a single ISAC transmitter, future 6G wireless networks are expected to incorporate densely deployed base stations (BSs). With the advancements in coordinated multi-point (CoMP) transmission [18], cloud radio access network [19], and cell-free multiple-input multiple-output (MIMO) [20], leveraging multiple BSs as cooperative ISAC transmitters serves as a promising natural architecture in further enhancing performance. On the one hand, there have been several works investigating coordinated beamforming among multiple BSs for enabling networked ISAC [21]–[23], in which different ISAC transmitters send independent information and sensing signals to communicate with their respective communication users (CUs) and perform joint target detection, estimation, or localization via multi-static or distributed MIMO sensing [24]. By cooperatively designing the coordinated beamforming vectors, ISAC transmitters not only effectively mitigate interference among CUs but also achieve enhanced cooperative multi-static sensing. For instance, [21] introduced a novel approach for coordinated ISAC in cellular networks, considering a beampattern optimization problem subject to communication signal-to-interference-plus-noise-ratio (SINR) constraints and

sensing receive power constraints. Furthermore, the authors in [22] explored a multi-antenna networked ISAC system, maximizing the detection probability under communication SINR requirements and power constraints via jointly optimizing the information and sensing beamforming. In [23], the authors considered the total power minimization problem in a networked ISAC system by collaboratively designing power control for different BSs.

On the other hand, the utilization of cell-free MIMO in ISAC has emerged as another viable realization of networked ISAC [25], where BSs or ISAC transmitters are connected to a central controller to share the communication and sensing data for joint transmission and collaborative sensing information processing [25]. Different from coordinated beamforming, cell-free ISAC can achieve enhanced communication performance by transforming harmful inter-cell interference into a part of useful information signals, and improve sensing performance via advanced sensing signal processing [20]. Inspired by these advantages, recent studies have investigated cell-free ISAC systems from different perspectives [26]–[29]. For example, the authors in [26] maximized the sum of communication and sensing rates by optimizing user association and power allocation, adopting a conjugate beamforming approach. Furthermore, in [28], the authors explored the multi-static sensing for cooperative target detection in cell-free ISAC, in which power allocation at different BSs is jointly optimized to maximize the sensing signal-to-noise ratio (SNR) while ensuring certain communication SINR requirements. Moreover, the authors in [27] optimized transmit information and sensing beamforming vectors at different BSs, in which the sensing SNR is maximized subject to the communication SINR constraints and the individual transmit power limitations at BSs.

The emergence of ISAC networks, however, introduces severe security concerns in both communication and sensing. First, to facilitate sensing, the optimized transmit information beams in ISAC systems are deliberately aimed at sensing targets to enhance sensing performance, thereby posing a potential risk of information leakage. This risk is particularly critical when sensing targets include suspicious entities such as eavesdropping unmanned aerial vehicles (UAVs) or other adversarial agents, escalating the potential of unauthorized interception of transmitted information. To address these concerns, several recent works have been developed to safeguard against unintended information leakage [30]–[33]. For example, to tackle communication security issues in ISAC systems, the authors in [30] explored the interplay between ISAC and secure communications to enable a multi-function wireless network integrating sensing, communication, and security. Moreover, the authors in [31] studied a secure ISAC system with a single eavesdropping target and multiple CUs, by considering line-of-sight (LoS) channel models with angle uncertainty for the eavesdropping target. The objective is to minimize the eavesdropping SINR at the target while satisfying the requirements for communication SINR at CUs and sensing beampatterns. Additionally, [32] proposed an optimization framework for robust secure resource allocation in a secure ISAC system, jointly optimizing transmit beamforming

and snapshot length, accounting for target angle uncertainty. In a related vein, the authors in [33] further considered the robust secure transmit beamforming problem for a single ISAC transmitter communicating with a single CU and detecting multiple targets, in which the transmit beampattern distortion is minimized under secrecy rate constraints for CUs with two different imperfect CSI scenarios.

Furthermore, the ISAC systems also encounter new sensing security threats, as the sensing information might be vulnerable to sensing eavesdroppers (see, e.g., [34]). By leveraging the sensing signals of ISAC systems, sensing eavesdroppers in ISAC systems may silently intercept sensing results without actively transmitting their own signals. Based on the intercepted sensing information, the adversary may infer the action of associated physical systems and possibly launch further actions jeopardizing system performance. Indeed, this passive eavesdropping on sensing information introduces additional privacy and security challenges, necessitating advanced mechanisms to ensure confidentiality and integrity of the sensed data [35], [36]. For instance, [35] investigated the precoder design in a single ISAC transmitter scenario based on sensing beampattern distortion. This study introduced a sensing adversary estimation framework tailored for estimating target location capitalizing on Bayesian inference. Besides, the authors in [36] further considered the precoder design in a cell-free ISAC system based on sensing SNR maximization. The study extended the sensing eavesdropper model via exploiting an expectation maximization method to eavesdrop target information. However, the prior research has not addressed the aspect of transmit design to safeguard sensing privacy [35], [36]. Furthermore, there is no existing work considering both communication and sensing security in cell-free ISAC systems, thus motivating our work.

This paper investigates a secure cell-free ISAC system, which comprises multiple ISAC transmitters collaboratively transmitting confidential information to multiple CUs, while concurrently performing joint target detection. We consider that there exist both information eavesdroppers and sensing eavesdroppers in this system, which aim to intercept confidential communication information and seek to extract sensing target information, respectively. The main results of this paper are listed as follows.

- Firstly, we introduce the system model for secure cell-free ISAC systems, including a communication framework and a multi-static sensing model that take into account the existence of sensing and information eavesdroppers. Our setup assumes that sensing receivers are equipped with knowledge of the transmitted signal, enabling effective clutter signal mitigation. By contrast, sensing eavesdroppers lack knowledge of the transmit signals, preventing them from mitigating the impacts caused by sensing clutters. In this scenario, we derive the detection probability at sensing receivers by exploiting the generalized likelihood ratio test (GLRT) detector. Besides, by assuming that eavesdroppers exploit signal power for target detection due to the lack of signal knowledge, we derive the closed-form eavesdropping probability underlining the interplay with different parameters.

- Next, we formulate the detection probability maximization problem, subject to the minimum SINR constraints at CUs for ensuring the successful transmission of confidential information. Meanwhile, the maximum tolerable SNR constraints at information eavesdroppers and the maximum eavesdropping probability constraints at sensing eavesdroppers are considered to safeguard information and sensing privacy, respectively. The formulated design problem, however, is highly difficult to solve, due to the inherent intractability caused by complex relationships between transmit beamforming vectors and legal sensing receivers/illegal sensing eavesdroppers, as well as the non-convex nature of communication SINR constraints. Fortunately, we achieve a globally optimal solution through a meticulously devised three-step approach. Initially, we reformulate the detection probabilities for legal sensing receivers and the eavesdropping probabilities for illegal sensing eavesdroppers to facilitate problem tractability. Subsequently, we relax the beamforming design problem by exploiting a semidefinite relaxation (SDR) approach [37], leading to a convex version that can be optimally solved with off-the-shelf toolboxes. Finally, rigorous proof of the relaxation's tightness is presented to verify the global optimality of the obtained solution.
- On the other hand, to cope with the needs in different practical scenarios, we present two alternative transmit beamforming designs based on the sensing SNR maximization and the coordinated beamforming, respectively. For the sensing SNR maximization design, our goal is to maximize the sensing power at the target direction, while in the coordinated beamforming design, each CU is associated with a specific BS for independent signal transmission. designs.
- Finally, numerical results are provided to validate the effectiveness of our proposed design, with comparisons against benchmarking sensing SNR maximization and coordinated beamforming. It is shown that via joint signal processing in the central controller, the proposed cell-free design effectively exploits the signal correlation among different transmitters, and also strategically utilizes the inherent sensing clutters to jam sensing eavesdroppers, thus ensuring the sensing security while improving the detection probability.

The remainder of this paper is organized as follows. Section II introduces the system model. Section III derives the detection probability and eavesdropping probability at sensing receivers and sensing eavesdroppers, respectively. Section IV formulates the joint transmit beamforming problem for secure cell-free ISAC, and develops a globally optimal solution to the formulated problem. Section V presents two alternative design approaches based on SNR maximization and coordinated beamforming, respectively. Section VI presents numerical results. Finally, Section VII concludes this paper.

*Notations:* Vectors and matrices are denoted by bold lower- and upper-case letters, respectively.  $\mathbb{C}^{N \times M}$  denotes the space of  $N \times M$  complex matrices.  $\mathbf{I}$  and  $\mathbf{0}$  represents an identity matrix and an all-zero matrix with appropriate dimensions,

respectively. For a square matrix  $\mathbf{A}$ ,  $\text{tr}(\mathbf{A})$  denotes its trace and  $\mathbf{A} \succeq \mathbf{0}$  means that  $\mathbf{A}$  is positive semi-definite. For a complex arbitrary-size matrix  $\mathbf{B}$ ,  $\mathbf{B}[i, j]$ ,  $\text{rank}(\mathbf{B})$ ,  $\mathbf{B}^T$ ,  $\mathbf{B}^H$ , and  $\mathbf{B}^c$  denote its  $(i, j)$ -th element, rank, transpose, conjugate transpose, and complex conjugate, respectively. For a vector  $\mathbf{a}$ ,  $\mathbf{a}[i]$  denotes its  $i$ -th element.  $\mathbb{E}(\cdot)$  denotes the statistical expectation.  $\|\cdot\|$  denotes the Euclidean norm of a vector.  $|\cdot|$ ,  $\text{Re}(\cdot)$ , and  $\text{Im}(\cdot)$  denote the absolute value, the real component, and the imaginary component of a complex entry.  $\mathcal{CN}(\mathbf{x}, \mathbf{Y})$  denotes a circularly symmetric complex Gaussian (CSCG) random vector with mean vector  $\mathbf{x}$  and covariance matrix  $\mathbf{Y}$ .  $\mathbf{A} \otimes \mathbf{B}$  represents the Kronecker product of two matrices  $\mathbf{A}$  and  $\mathbf{B}$ .  $\text{blkdiag}(\cdot)$  constructs a block diagonal matrix with its entities.  $\frac{\partial(\cdot)}{\partial}$  denotes the operator of a partial derivative.

## II. SYSTEM MODEL

We consider a secure cell-free ISAC system as shown in Fig. 1, which comprises  $M_t$  ISAC transmitters,  $M_r$  sensing receivers,  $K$  single-antenna CUs, as well as  $L$  single-antenna information eavesdroppers and  $Q$  sensing eavesdroppers. Let  $\mathcal{M}_t \triangleq \{1, \dots, M_t\}$ ,  $\mathcal{M}_r \triangleq \{1, \dots, M_r\}$ ,  $\mathcal{K} \triangleq \{1, \dots, K\}$ ,  $\mathcal{L} \triangleq \{1, \dots, L\}$ , and  $\mathcal{Q} \triangleq \{1, \dots, Q\}$  denote the sets of ISAC transmitters, sensing receivers, CUs, information eavesdroppers, and sensing eavesdroppers, respectively. Without loss of generality, we assume that each ISAC transmitter, sensing receiver, and sensing eavesdropper in our system is equipped with an array of  $N$  antennas.

In this ISAC system, the objective is to address the communication requirements of the  $K$  CUs while simultaneously conducting sensing operations in a specific area of interest. The central controller coordinates the ISAC transmitters and sensing receivers to ensure the security in the cell-free ISAC system. It is assumed that all ISAC transmitters and sensing receivers achieve perfect synchronization facilitated by the central controller [27], [28]. Additionally, we consider a basic scenario in which there is no collaboration among any sensing or information eavesdroppers.

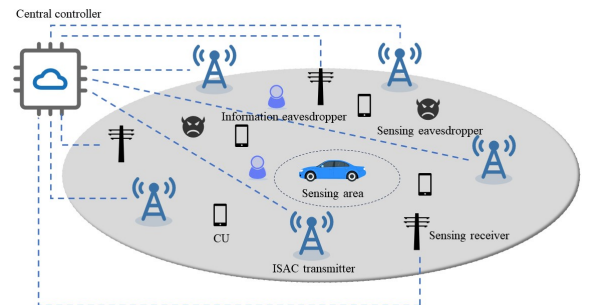


Fig. 1. Illustration of the secure cell-free ISAC system.

### A. Communication Model

In our framework, we focus on the ISAC transmission over a period of  $T$  symbols, where  $T$  is assumed to be

sufficiently large. We denote  $\hat{s}_k^I(t) \in \mathbb{C}$  as the desired information signal for CU  $k \in \mathcal{K}$  in the  $t$ -th symbol. We model  $\hat{s}_k^I(t)$ 's as independent and identically distributed (i.i.d.) CSCG random variables each with zero mean and unit variance, i.e.,  $\hat{s}_k^I(t) \sim \mathcal{CN}(0, 1)$ . Let  $\hat{\mathbf{w}}_{i,k} \in \mathbb{C}^{N \times 1}$  denote the transmit beamforming vector at transmitter  $i \in \mathcal{M}_t$  for CU  $k$ . We define  $\mathbf{w}_k \in \mathbb{C}^{NM_t \times 1}$  as the beamforming vector spanning all the  $M_t$  ISAC transmitters for CU  $k \in \mathcal{K}$ , i.e.,

$$\mathbf{w}_k = [\hat{\mathbf{w}}_{1,k}^T, \dots, \hat{\mathbf{w}}_{M_t,k}^T]^T. \quad (1)$$

Moreover, we assume that all ISAC transmitters collaboratively employ dedicated sensing signals to fully exploit the available DoFs for the purpose of sensing [11]. Let  $\hat{s}_i^S(t)$  denote the dedicated sensing signal at ISAC transmitter  $i \in \mathcal{M}_t$ . In this context, we define  $\mathbf{s}^S(t) \in \mathbb{C}^{NM_t \times 1}$  as the dedicated sensing signal in the  $t$ -th symbol, spanning all the  $M_t$  ISAC transmitters, i.e.,

$$\mathbf{s}^S(t) = [(\hat{s}_1^S(t))^T, \dots, (\hat{s}_{M_t}^S(t))^T]^T. \quad (2)$$

We define the covariance of the dedicated sensing signal  $\mathbf{s}^S(t)$  as

$$\mathbf{S} = \mathbb{E}(\mathbf{s}^S(t)(\mathbf{s}^S(t))^H). \quad (3)$$

Without loss of generality, we assume that  $\mathbf{S}$  is a general-rank matrix, serving as an optimization variable in our system. Typically, the number of dedicated sensing beams is determined by the rank of  $\mathbf{S}$ . Consequently, the transmitted signal at ISAC transmitter  $i \in \mathcal{M}_t$  is expressed as [28]

$$\mathbf{x}_i(t) = \sum_{k=1}^K \hat{\mathbf{w}}_{i,k} \hat{s}_k^I(t) + \hat{s}_i^S(t). \quad (4)$$

Let  $\mathbf{x}(t) = [\mathbf{x}_1^T(t), \dots, \mathbf{x}_{M_t}^T(t)]^T$  denote the accumulated transmitted signal across all the  $M_t$  ISAC transmitters. We define the transmit covariance across all the ISAC transmitters as

$$\mathbf{R} = \mathbb{E}(\mathbf{x}(t)\mathbf{x}^H(t)) = \sum_{k=1}^K \mathbf{w}_k \mathbf{w}_k^H + \mathbf{S}. \quad (5)$$

Let  $\hat{\mathbf{h}}_{i,k} \in \mathbb{C}^{N \times 1}$  denote the channel vector between CU  $k \in \mathcal{K}$  and ISAC transmitter  $i \in \mathcal{M}_t$ . Here, we introduce the overall channel from CU  $k \in \mathcal{K}$  to all  $M_t$  transmitters as  $\mathbf{h}_k \in \mathbb{C}^{NM_t \times 1}$ , i.e.,

$$\mathbf{h}_k = [\hat{\mathbf{h}}_{1,k}^T, \dots, \hat{\mathbf{h}}_{M_t,k}^T]^T. \quad (6)$$

As a result, the received signal at CU  $k \in \mathcal{K}$  is expressed as (7) at the top of the next page, which consists of three main components, i.e., desired signal, multi-user interference, and sensing signal interference. Here,  $n_k(t)$  is the independent Gaussian noise with a zero mean and variance  $\sigma^2$  at CU  $k \in \mathcal{K}$  in the  $t$ -th symbol, i.e.,  $n_k(t) \sim \mathcal{CN}(0, \sigma^2)$ . As such, the received SINR at the receiver of CU  $k \in \mathcal{K}$  is given in (8) at the top of the next page. It is worth noting that the interference term in (8) stems from two aspects, i.e., multi-user interference and sensing signal interference [27].

## B. Information Eavesdropping

In this subsection, we focus on the information eavesdropping model, in which information eavesdropper  $l \in \mathcal{L}$  may attempt to intercept confidential information intended for any CU  $k \in \mathcal{K}$ . Let  $\hat{\mathbf{g}}_{i,l} \in \mathbb{C}^{N \times 1}$  represent the channel vector from ISAC transmitter  $i \in \mathcal{M}_t$  to information eavesdropper  $l \in \mathcal{L}$ . Let  $\mathbf{g}_l \in \mathbb{C}^{NM_t \times 1}$  denote the accumulated channel from all ISAC  $M_t$  transmitters to eavesdropper  $l$ , i.e.,

$$\mathbf{g}_l = [\hat{\mathbf{g}}_{1,l}^T, \dots, \hat{\mathbf{g}}_{M_t,l}^T]^T. \quad (9)$$

The received signal at information eavesdropper  $l \in \mathcal{L}$  is given by (10) at the top of next page, in which  $\tilde{n}_l(t)$  denotes the noise at the receiver that is an i.i.d. CSCG random variable with a zero mean and variance  $\sigma^2$ . It is assumed that there is no cooperation among different information eavesdroppers.

Notice that if information eavesdropper  $l \in \mathcal{L}$  is aware of the channel  $\mathbf{g}_l$  and transmitted sensing signal sequence  $\{\hat{s}_i^S(t)\}$ , then it may be able to effectively cancel the interference caused by sensing signals via advanced signal processing [38]. Subsequently, by employing successive interference cancellation (SIC) [39], each information eavesdropper can proceed to cancel the information signal intended for other CUs (if they are decoded) before attempting to decode the signal of CU  $k \in \mathcal{K}$ . As a result, we impose the worst-case assumption that information eavesdropper  $l \in \mathcal{L}$  can perfectly cancel the information signal for other CUs and the dedicated sensing signal. In this case and under the assumption without cooperation among different information eavesdroppers, the received eavesdropping SNR at information eavesdropper  $l \in \mathcal{L}$  for intercepting signals for CU  $k \in \mathcal{K}$  is given by

$$\tilde{\gamma}_{l,k}(\{\mathbf{w}_k\}, \mathbf{S}) = \frac{|\mathbf{g}_l^H \mathbf{w}_k|^2}{\sigma^2}. \quad (11)$$

To protect the communication security, in this paper we need to ensure that the information eavesdropping SNR  $\tilde{\gamma}_{l,k}(\{\mathbf{w}_k\}, \mathbf{S})$  at any information eavesdropper  $l \in \mathcal{L}$  should not exceed a given threshold for all CU  $k \in \mathcal{K}$ .

## C. Multi-static Sensing

In this subsection, we consider the multi-static sensing model within this cell-free network. In this scenario, the central controller aggregates the received signals from all  $M_r$  receivers to perform joint target detection. First, we assume that the sensing receivers are aware of the transmitted signal  $\mathbf{x}_i(t)$  and the environmental information, including clutters and LoS path. As such, the sensing receivers possess the capability to efficiently mitigate signals originating from clutters and LoS path [28]. In case that the target is present, the received signal at sensing receiver  $j \in \mathcal{M}_r$  in the  $t$ -th symbol is expressed as

$$\mathbf{r}_j(t) = \sum_{i=1}^{M_t} \alpha_{i,j} \mathbf{a}_r(\varphi_j) \mathbf{a}_t^H(\theta_i) \mathbf{x}_i(t) + \bar{\mathbf{n}}_j(t), \quad (12)$$

where  $\alpha_{i,j} \in \mathbb{C}$  represents the complex coefficient characterizing the influence of path-loss and the target radar cross section (RCS) between ISAC transmitter  $i \in \mathcal{M}_t$  and sensing receiver

$$y_k(t) = \sum_{i=1}^{M_t} \hat{\mathbf{h}}_{i,k}^H \mathbf{x}_i(t) + n_k(t) = \underbrace{\mathbf{h}_k^H \mathbf{w}_k \hat{s}_k^I(t)}_{\text{Desired signal}} + \underbrace{\sum_{j=1, j \neq k}^K \mathbf{h}_k^H \mathbf{w}_j \hat{s}_j^I(t)}_{\text{Multi-user interference}} + \underbrace{\mathbf{h}_k^H \mathbf{s}^S(t)}_{\text{Sensing signal interference}} + n_k(t) \quad (7)$$

$$\gamma_k(\{\mathbf{w}_k\}, \mathbf{S}) = \frac{|\sum_{i=1}^{M_t} \hat{\mathbf{h}}_{i,k}^H \hat{\mathbf{w}}_{i,k}|^2}{\sum_{j=1, j \neq k}^K |\sum_{i=1}^{M_t} \hat{\mathbf{h}}_{i,k}^H \hat{\mathbf{w}}_{i,j}|^2 + \mathbb{E}(|\sum_{i=1}^{M_t} \hat{\mathbf{h}}_{i,k}^H \hat{s}_i^S(t)|^2) + \sigma^2} = \frac{|\mathbf{h}_k^H \mathbf{w}_k|^2}{\sum_{j=1, j \neq k}^K |\mathbf{h}_k^H \mathbf{w}_j|^2 + \mathbf{h}_k^H \mathbf{S} \mathbf{h}_k + \sigma^2}. \quad (8)$$

$$\tilde{y}_l(t) = \sum_{i=1}^{M_t} \hat{\mathbf{g}}_{i,l}^H \mathbf{x}_i(t) = \mathbf{g}_l^H \mathbf{w}_k \hat{s}_k^I(t) + \sum_{j=1, j \neq k}^K \mathbf{g}_l^H \mathbf{w}_j \hat{s}_j^I(t) + \mathbf{g}_l^H \mathbf{s}^S(t) + \tilde{n}_l(t). \quad (10)$$

$j \in \mathcal{M}_r$ , which is an unknown deterministic parameter. Additionally,  $\theta_i$  denotes the angle of departure (AoD) from ISAC transmitter  $i \in \mathcal{M}_t$  to the target and  $\varphi_j$  denotes the angle of arrival (AoA) from the target to sensing receiver  $j \in \mathcal{M}_r$ . Furthermore,  $\mathbf{a}_t(\cdot)$  and  $\mathbf{a}_r(\cdot)$  represent the transmit and receive steering vectors, respectively, and  $\tilde{\mathbf{n}}_j$  represents the Gaussian noise at sensing receiver  $j \in \mathcal{M}_r$ , with each element having a zero mean and a variance of  $\sigma_s^2$ . For notational convenience, we denote

$$\phi_{i,j}(t) \triangleq \mathbf{a}_r(\varphi_j) \mathbf{a}_t^H(\theta_i) \mathbf{x}_i(t) \quad (13)$$

as the signal received by sensing receiver  $j \in \mathcal{M}_r$  from ISAC transmitter  $i \in \mathcal{M}_t$  reflected by the target excluding the influence of  $\alpha_{i,j}$ . It is worth noting that  $\phi_{i,j}(t)$  is assumed to be perfectly known at sensing receivers and thus can be utilized to design a target detector. Let  $\Phi_j(t) = [\phi_{1,j}(t), \dots, \phi_{M_t,j}(t)] \in \mathbb{C}^{N \times M_t}$  denote the received signal at sensing receiver  $j \in \mathcal{M}_r$  from all ISAC transmitters. The reflected signal at all sensing receivers from all ISAC transmitters in the  $t$ -th symbol is given as

$$\Phi(t) = \text{blkdiag}(\Phi_1(t), \dots, \Phi_{M_r}(t)) \in \mathbb{C}^{NM_r \times M_t M_r}. \quad (14)$$

As a result, the concatenated received signal over all  $M_r$  sensing receivers at the  $t$ -th symbol is given by

$$\phi_s(t) = \Phi(t) \boldsymbol{\alpha} + \mathbf{n}_s(t), \quad (15)$$

where  $\boldsymbol{\alpha} = [\alpha_{1,1}, \dots, \alpha_{1,M_r}, \dots, \alpha_{M_t,1}, \dots, \alpha_{M_t,M_r}]^T$ . Furthermore, define  $\Psi = [\Phi^T(1), \dots, \Phi^T(T)]^T \in \mathbb{C}^{NM_r T \times M_t M_r}$  as the concatenated signal formed by  $\Phi(t)$  over total  $T$  symbols. Let  $\mathbf{r}_S \in \mathbb{C}^{NM_r T \times 1}$  denote the received concatenated signal at all the  $M_r$  sensing receivers over  $T$  symbols, which is given by

$$\mathbf{r}_S = \Psi \boldsymbol{\alpha} + \mathbf{n}_s, \quad (16)$$

where  $\mathbf{n}_s \in \mathbb{C}^{NM_r T \times 1}$  denotes the noise at the sensing receivers with  $\mathbf{n}_s \sim \mathcal{CN}(\mathbf{0}, \sigma_s^2 \mathbf{I})$ .

Let null hypothesis  $\mathcal{H}_0$  represent that there is no target in the sensing area, and the alternative hypothesis  $\mathcal{H}_1$  represent the existence of the target. As a result, we formulate the hypothesis as

$$\begin{cases} \mathcal{H}_0: & \mathbf{r}_S = \mathbf{n}_s, \\ \mathcal{H}_1: & \mathbf{r}_S = \Psi \boldsymbol{\alpha} + \mathbf{n}_s. \end{cases} \quad (17)$$

Let  $p_D(\{\mathbf{w}_k\}, \mathbf{S})$  denote the detection probability at sensing receivers based on (17), which is a function of design variables  $\{\mathbf{w}_k\}$  and  $\mathbf{S} = \mathbb{E}(\mathbf{s}^S(t)(\mathbf{s}^S(t))^H)$  to be determined in Section III.

#### D. Sensing Eavesdropping

In this subsection, we investigate the sensing eavesdropping model. Since the transmitted signal  $\mathbf{x}(t)$  is confidential, these sensing eavesdroppers are assumed to lack knowledge about  $\mathbf{x}(t)$ , rendering sensing techniques requiring  $\mathbf{x}(t)$  inapplicable. Generally, the sensing eavesdroppers' goal is to detect the transmitted power from a specific direction to perform target detection. In this context, we assume that sensing eavesdropper  $q \in \mathcal{Q}$  adopts receive beamforming with a beamforming vector  $\mathbf{a}_r^H(\omega_q)$  to detect the received power along the target direction, similar to a passive radar technique [40], where  $\omega_q$  denotes the AoD from the target to sensing eavesdropper  $q \in \mathcal{Q}$ . Let  $\mathbf{U}_{i,q} \in \mathbb{C}^{N \times N}$  denote the clutter channel from ISAC transmitter  $i \in \mathcal{M}_t$  to sensing eavesdropper  $q \in \mathcal{Q}$ . We assume that the clutter information is available to both the central controller and sensing eavesdroppers. However, as the sensing eavesdroppers are not aware of the transmitted signal  $\mathbf{x}(t)$ , they cannot cancel the resulted interference from clutters. Let  $\eta_{i,q} \in \mathbb{C}$  represent the complex coefficient from ISAC transmitter  $i \in \mathcal{M}_t$  to sensing eavesdropper  $q \in \mathcal{Q}$  characterizing the influence of path-loss and target RCS. Consequently, after applying receive beamformer  $\mathbf{a}_r^H(\omega_q)$ , the received signal by sensing eavesdropper  $q \in \mathcal{Q}$  in the  $t$ -th symbol is given by

$$\begin{aligned} \tilde{r}_q(t) &= \mathbf{a}_r^H(\omega_q) \left( \sum_{i=1}^{M_t} \eta_{i,q} \mathbf{a}_r(\omega_q) \mathbf{a}_t^H(\theta_i) \mathbf{x}_i(t) \right. \\ &\quad \left. + \underbrace{\sum_{i=1}^{M_t} \mathbf{U}_{i,q}^H \mathbf{x}_i(t)}_{\text{clutters}} + \hat{\mathbf{n}}_q(t) \right), \end{aligned} \quad (18)$$

where  $\hat{\mathbf{n}}_q(t) \in \mathbb{C}^{N \times 1}$  is the noise with  $\hat{\mathbf{n}}_q(t) \sim \mathcal{CN}(\mathbf{0}, \sigma_s^2 \mathbf{I})$ . For convenience, we rewrite (18) as

$$\tilde{r}_q(t) = \mathbf{a}_q^H \mathbf{x}(t) + \mathbf{u}_q^H \mathbf{x}(t) + \mathbf{a}_r^H(\omega_q) \hat{\mathbf{n}}_q(t), \quad (19)$$

where  $\mathbf{a}_q = [N\eta_{1,n}\mathbf{a}_t^H(\theta_1), \dots, N\eta_{M_t,n}\mathbf{a}_t^H(\theta_{M_t})]^H$  is the equivalent steering vector, and  $\mathbf{u}_q = [\mathbf{a}_r^H(\omega_q)\mathbf{U}_{1,n}^H, \dots, \mathbf{a}_r^H(\omega_q)\mathbf{U}_{M_t,n}^H]^H$  is the equivalent clutter channel. Let  $\tilde{\mathbf{n}}_q(t) = \mathbf{a}_r^H(\omega_q)\hat{\mathbf{n}}_q(t) \sim \mathcal{CN}(0, N\sigma_s^2)$  denote the equivalent noise.

Let the null hypothesis  $\tilde{\mathcal{H}}_0$  represent that there is no target in the sensing area, while the alternative hypothesis  $\tilde{\mathcal{H}}_1$  represent the existence of the target. As a result, we formulate the hypothesis as

$$\begin{cases} \tilde{\mathcal{H}}_0 : \tilde{r}_q(t) = \mathbf{u}_q^H \mathbf{x}(t) + \tilde{\mathbf{n}}_q(t), \\ \tilde{\mathcal{H}}_1 : \tilde{r}_q(t) = \mathbf{a}_q^H \mathbf{x}(t) + \mathbf{u}_q^H \mathbf{x}(t) + \tilde{\mathbf{n}}_q(t). \end{cases} \quad (20)$$

Let  $\tilde{p}_q(\{\mathbf{w}_k\}, \mathbf{S})$  denote the eavesdropping probability at sensing eavesdropper  $q \in \mathcal{Q}$  based on (20), which will be derived in Section III shortly.

### III. DETECTION AND EAVESDROPPING PROBABILITIES

Typically, the detection probability  $p_D(\{\mathbf{w}_k\}, \mathbf{S})$  and the eavesdropping probability  $\tilde{p}_q(\{\mathbf{w}_k\}, \mathbf{S})$  are both intricate functions with respect to (w.r.t.) design variables  $\{\mathbf{w}_k\}$  and  $\mathbf{S}$ , posing tremendous challenges in both modeling and optimization w.r.t.  $\{\mathbf{w}_k\}$  and  $\mathbf{S}$ . In this section, we establish the relationships between these probabilities and design variables  $\{\mathbf{w}_k\}$  and  $\mathbf{S}$ .

#### A. Detection Probability at Sensing Receivers

To begin with, we derive the detection probability at the sensing receivers based on the multi-static sensing model in (17). Here, we treat  $\alpha$  as the unknown but deterministic parameters. Note that  $\alpha \neq \mathbf{0}$  represents that there is target in the interested area. In this case, the detection problem can be modeled as a linear model. Following the signal detection in a noisy scenario [41], the hypothesis in (17) is equivalently reformulated as

$$\begin{cases} \mathcal{H}_0 : \boldsymbol{\mu}^T \alpha = 0, \\ \mathcal{H}_1 : \boldsymbol{\mu}^T \alpha \neq 0, \end{cases} \quad (21)$$

where  $\boldsymbol{\mu} = \mathbf{1} \in \mathbb{C}^{M_t M_r \times 1}$ . Given that parameters  $\alpha$  is unknown and based on the expression of  $\Phi(t)$  in (14), we proceed to apply the GLRT detector [41] based on the hypothesis in (21).

**Proposition 1.** The GLRT for (21) is given as

$$\nu(\mathbf{Y}) = \frac{|\boldsymbol{\mu}^T \hat{\alpha}_1|^2}{\sigma_s^2 \boldsymbol{\mu}^T (\Psi^H \Psi)^{-1} \boldsymbol{\mu}}, \quad (22)$$

where  $\hat{\alpha}_1 = (\Psi^H \Psi)^{-1} \Psi^H \mathbf{r}_S$ . Let  $\Xi$  denote the test threshold, the false alarm, and detection probabilities at sensing receivers are respectively given by

$$p_{\text{FA}} = \Upsilon_{\chi^2}(\Xi), \quad (23)$$

$$p_D(\{\mathbf{w}_k\}, \mathbf{S}) = \Upsilon_{\tilde{\chi}^2(\lambda(\{\mathbf{w}_k\}, \mathbf{S}))}(\Xi), \quad (24)$$

where  $\chi^2(\cdot)$  is the central Chi-square distribution,  $\tilde{\chi}^2(\lambda)$  is the non-central Chi-square distribution with a non-centrality parameter  $\lambda(\{\mathbf{w}_k\}, \mathbf{S}) = \frac{|\boldsymbol{\mu}^T \alpha|^2}{\sigma_s^2 \boldsymbol{\mu}^T (\Psi^H \Psi)^{-1} \boldsymbol{\mu}}$ , and  $\Upsilon$  represents

the right-tailed distribution. Here,  $\lambda(\{\mathbf{w}_k\}, \mathbf{S})$  is a function of  $\Psi$  and thus a function of optimization variables  $\{\mathbf{w}_k\}$  and  $\mathbf{S}$ .

*Proof.* Please refer to Appendix A.  $\square$

#### B. Eavesdropping Probability at Sensing Eavesdroppers

Next, we consider the eavesdropping probability at sensing eavesdropper  $q \in \mathcal{Q}$ . Since we assume that the transmitted signal  $\mathbf{x}(t)$  is confidential, the sensing eavesdropper does not know  $\mathbf{x}(t)$ . As a result, the sensing eavesdropper can only perform energy detection to decide whether the target exists, i.e., the detector is given as  $|\tilde{r}_q(t)|^2$  [42]. Consequently, the likelihood functions of  $y_q(t)$  under  $\tilde{\mathcal{H}}_0$  and  $\tilde{\mathcal{H}}_1$  are respectively given by

$$\begin{aligned} p_0(\tilde{r}_q(t)) &= \frac{1}{\pi \zeta_q(\{\mathbf{w}_k\}, \mathbf{S})} \exp\left(-\frac{|\tilde{r}_q(t)|^2}{\zeta_q(\{\mathbf{w}_k\}, \mathbf{S})}\right), \\ p_1(\tilde{r}_q(t)) &= \frac{1}{\pi \beta_q(\{\mathbf{w}_k\}, \mathbf{S})} \exp\left(-\frac{|\tilde{r}_q(t)|^2}{\beta_q(\{\mathbf{w}_k\}, \mathbf{S})}\right), \end{aligned} \quad (25)$$

where we define  $\zeta_q(\{\mathbf{w}_k\}, \mathbf{S}) = \mathbf{u}_q^H \mathbf{R} \mathbf{u}_q + N\sigma^2$  and  $\beta_q(\{\mathbf{w}_k\}, \mathbf{S}) = (\mathbf{a}_q + \mathbf{u}_q)^H \mathbf{R} (\mathbf{a}_q + \mathbf{u}_q) + N\sigma^2$ , with  $\mathbf{R}$  denoting the covariance matrix in (5). In accordance with the hypothesis in (20), Proposition 2 provides the maximum target detection probability via the Neyman-Pearson criterion under the optimal threshold.

**Proposition 2.** The maximum target detection probability under the optimal threshold is given as

$$\tilde{p}_q(\{\mathbf{w}_k\}, \mathbf{S}) = \left(\frac{\beta_q(\{\mathbf{w}_k\}, \mathbf{S})}{\zeta_q(\{\mathbf{w}_k\}, \mathbf{S})}\right)^{-\frac{\zeta_n(\{\mathbf{w}_k\}, \mathbf{S})}{\beta_q(\{\mathbf{w}_k\}, \mathbf{S}) - \zeta_n(\{\mathbf{w}_k\}, \mathbf{S})}}. \quad (26)$$

*Proof.* Please refer to Appendix B.  $\square$

*Remark 1.* It is important to compare the detection probability in Proposition 1 versus the eavesdropping probability in Proposition 2. Notice that sensing receivers are aware of the transmitted signal  $\mathbf{x}(t)$ , but sensing eavesdroppers do not have such information. As a result, sensing receivers are able to design a detector via jointly exploiting the knowledge of  $\mathbf{x}(t)$  in received signal  $\mathbf{r}_S$ , but each sensing eavesdropping can only perform target detection independently via detecting the received signal power along the target direction. On the other hand, sensing receivers have the capability to cancel clutters, while sensing eavesdroppers do not possess this capability. As such, the inherent clutters result in interference towards sensing eavesdroppers only, which can be utilized to jam sensing eavesdroppers for preserving the sensing data privacy, which will be discussed in the subsequent section.

### IV. JOINT TRANSMIT BEAMFORMING DESIGN FOR SECURE CELL-FREE ISAC

In this section, we first formulate a joint transmit beamforming problem for the secure cell-free ISAC system. Our objective is to maximize the detection probability subject to the minimum SINR constraints at the CUs. Meanwhile, the formulation considers the maximum SNR constraints at information eavesdroppers to ensure the confidentiality of information transmission and the maximum detection probability constraints at sensing eavesdroppers to maintain the sensing privacy. Following this, we introduce a three-step approach to achieve a globally optimal solution.

### A. Problem Formulation

In this subsection, our goal is to maximize the legal detection probability, as defined in Proposition 1, while ensuring that the CUs meet a minimum SINR threshold. This is achieved through the optimization of both the transmit information beamformers  $\{\mathbf{w}_k\}$  and the dedicated sensing covariance  $\mathbf{S}$ . Furthermore, the transmission of each ISAC transmitter is constrained by a maximum power budget  $P$ . For ease of presentation, let  $\mathbf{A}_i \in \mathbb{C}^{N \times N M_t}$  denote an auxiliary binary matrix to extract  $\hat{\mathbf{w}}_{i,k}$  from  $\mathbf{w}_k$ , which is composed of  $M_t$  individual  $N \times N$  matrices arranged horizontally. Within this composite matrix, only the  $i$ -th segment contains an identity matrix, while all other segments consist of zeros, i.e.,

$$\mathbf{A}_i = [\mathbf{0}, \dots, \underbrace{\mathbf{I}}_{\text{the } i\text{-th matrix}}, \dots, \mathbf{0}]. \quad (27)$$

In this case, the transmit power constraint at ISAC transmitter  $i \in \mathcal{M}_t$  is given by

$$\mathbb{E}(\mathbf{x}_i^H(t)\mathbf{x}_i(t)) = \text{tr} \left( \mathbf{A}_i \left( \sum_{k=1}^K \mathbf{w}_k \mathbf{w}_k^H + \mathbf{S} \right) \mathbf{A}_i^H \right) \leq P. \quad (28)$$

Let  $\Gamma$ ,  $\Omega$ , and  $\Lambda$  denote the required minimum communication SINR threshold for the CUs, the maximum information eavesdropping SNR threshold for the information eavesdroppers, and the maximum eavesdropping sensing probability threshold for the sensing eavesdroppers, respectively. Consequently, the joint transmit beamforming problem for secure cell-free ISAC is formulated as

$$\begin{aligned} \text{(P1)} : \quad & \max_{\{\mathbf{w}_k\}, \mathbf{S}} \Upsilon_{\tilde{\chi}^2(\lambda(\{\mathbf{w}_k\}, \mathbf{S}))}(\bar{\Xi}) \\ & \text{s.t.} \quad \gamma_k(\{\mathbf{w}_k\}, \mathbf{S}) \geq \Gamma, \forall k \in \mathcal{K}, \quad (29a) \\ & \quad \tilde{\gamma}_{l,k}(\{\mathbf{w}_k\}, \mathbf{S}) \leq \Omega, \forall l \in \mathcal{L}, k \in \mathcal{K}, \quad (29b) \\ & \quad \tilde{p}_q(\{\mathbf{w}_k\}, \mathbf{S}) \leq \Lambda, \forall q \in \mathcal{Q}, \quad (29c) \\ & \quad \text{tr} \left( \mathbf{A}_i \left( \sum_{k=1}^K \mathbf{w}_k \mathbf{w}_k^H + \mathbf{S} \right) \mathbf{A}_i^H \right) \leq P, \forall i \in \mathcal{M}_t, \quad (29d) \\ & \quad \mathbf{S} \succeq \mathbf{0}. \quad (29e) \end{aligned}$$

It is important to note that problem (P1) exhibits a high degree of non-convexity, mainly stemming from the non-convex and non-smooth nature of the objective function and the constraints presented in (29a), (29b), and (29c). Therefore, it is challenging to solve. In the subsequent subsection, we present an effective approach to address these challenges and obtain a globally optimal solution to problem (P1).

### B. Optimal Solution to Problem (P1)

In this subsection, we present a three-step approach to obtain a globally optimal solution to problem (P1). Initially, we simplify the detection probability and eavesdropping probability to enhance problem tractability. Subsequently, we reformulate the problem by adopting the SDR method [37], such that the convex SDR version can be optimally solved via off-the-shelf toolboxes. Finally, we rigorously verify the tightness of the adopted SDR to ensure the global optimality of the obtained solution.

1) *Problem Reformulation:* To begin with, we exploit the detection probability expression in Proposition 1 and establish its equivalent form that is tractable for optimization. Despite the non-smooth nature of the detection probability expression in Proposition 1 w.r.t.  $\lambda(\{\mathbf{w}_k\}, \mathbf{S})$ , it is observed that an increase in the non-centrality parameter  $\lambda(\{\mathbf{w}_k\}, \mathbf{S})$  results in an increase in the right-tail probability for a non-central chi-square distribution, given a specific threshold. This is because that as  $\lambda(\{\mathbf{w}_k\}, \mathbf{S})$  increases, the entire non-central chi-square distribution shifts to the right, leading to an augmentation in the right-tail probability. Consequently, we establish that maximizing the detection probability  $p_D(\{\mathbf{w}_k\}, \mathbf{S})$  is equivalent to maximizing the non-centrality parameter  $\lambda(\{\mathbf{w}_k\}, \mathbf{S})$ , which is further equivalent to minimizing  $\boldsymbol{\mu}^T (\boldsymbol{\Psi}^H \boldsymbol{\Psi})^{-1} \boldsymbol{\mu}$  in the denominator.

Next, we consider the expression  $\boldsymbol{\Psi}^H \boldsymbol{\Psi}$ . Recall that  $\boldsymbol{\Psi} = [\boldsymbol{\Phi}^T(1), \dots, \boldsymbol{\Phi}^T(T)]^T$  and  $\boldsymbol{\Phi}(t) = \text{blkdiag}(\boldsymbol{\Phi}_1(t), \dots, \boldsymbol{\Phi}_{M_r}(t))$ . As such, we derive  $\boldsymbol{\Psi}^H \boldsymbol{\Psi}$  as

$$\boldsymbol{\Psi}^H \boldsymbol{\Psi} = \sum_{t=1}^T \text{blkdiag}(\boldsymbol{\Phi}_1^H(t)\boldsymbol{\Phi}_1(t), \dots, \boldsymbol{\Phi}_{M_r}^H(t)\boldsymbol{\Phi}_{M_r}(t)). \quad (30)$$

Notice that the correlation of the received signal  $\boldsymbol{\Phi}_j^H(t)\boldsymbol{\Phi}_j(t)$  at sensing receiver  $j \in \mathcal{M}_r$  is given by

$$\boldsymbol{\Phi}_j^H(t)\boldsymbol{\Phi}_j(t) = \begin{bmatrix} \phi_{1,j}^H(t)\phi_{1,j}(t) & \dots & \phi_{1,j}^H(t)\phi_{M_t,j}(t) \\ \dots & \dots & \dots \\ \phi_{M_t,j}^H(t)\phi_{1,j}(t) & \dots & \phi_{M_t,j}^H(t)\phi_{M_t,j}(t) \end{bmatrix}. \quad (31)$$

Also notice that for the received signals from ISAC transmitters  $m \in \mathcal{M}_t$  and  $n \in \mathcal{M}_t$  at sensing receiver  $j \in \mathcal{M}_r$ , it follows that

$$\begin{aligned} \sum_{t=1}^T \phi_{m,j}^H(t)\phi_{n,j}(t) &= N \sum_{t=1}^T \mathbf{x}_m^H(t)\mathbf{a}_t(\theta_m)\mathbf{a}_t^H(\theta_n)\mathbf{x}_n(t) \\ &\stackrel{(a)}{=} TN \text{tr}(\mathbf{a}_t(\theta_m)\mathbf{a}_t^H(\theta_n)\mathbf{R}_{m,n}), \quad (32) \end{aligned}$$

where  $\mathbf{R}_{m,n} = \mathbb{E}(\mathbf{x}_n(t)\mathbf{x}_m^H(t))$  and equality (a) holds due to the fact the statistical covariance matrix  $\mathbf{R}_{m,n}$  is equivalent to the sample covariance matrix when the number  $T$  of symbols is sufficiently large [4]. As a result, by combining (30), (31), and (32), we rewrite  $\boldsymbol{\Psi}^H \boldsymbol{\Psi}$  as

$$\boldsymbol{\Psi}^H \boldsymbol{\Psi} = \text{blkdiag}(\underbrace{\mathbf{R}_\Phi}_{M_r}, \dots, \mathbf{R}_\Phi), \quad (33)$$

where  $\mathbf{R}_\Phi \in \mathbb{C}^{M_t \times M_t}$  and

$$\mathbf{R}_\Phi[m, n] = TN \text{tr}(\mathbf{a}_t(\theta_m)\mathbf{a}_t^H(\theta_n)\mathbf{A}_m \mathbf{R} \mathbf{A}_n^H). \quad (34)$$

As a result, maximizing the detection probability expression in Proposition 1 is shown to be equivalent to minimizing the following tractable and equivalent form<sup>1</sup>:

$$\boldsymbol{\mu}^T (\boldsymbol{\Psi}^H \boldsymbol{\Psi})^{-1} \boldsymbol{\mu}. \quad (35)$$

<sup>1</sup>It is insightful to discuss the covariance matrix  $\mathbf{R}_\Phi$  in (34). The diagonal elements in  $\mathbf{R}_\Phi$  represent the transmitted power directed towards the sensing target at ISAC transmitters. Meanwhile, the non-diagonal elements in  $\mathbf{R}_\Phi$  capture the covariance of transmitted signals from different ISAC transmitters. Notably, the covariance of transmitted signals from various ISAC transmitters should be properly designed together with the power directed towards the target to enhance detection performance.

Next, we address the non-convex eavesdropping probability in constraints (29c), which is given in the following form:

$$\tilde{p}_q(\{\mathbf{w}_k\}, \mathbf{S}) = \left( \frac{\beta_q(\{\mathbf{w}_k\}, \mathbf{S})}{\zeta_n(\{\mathbf{w}_k\}, \mathbf{S})} \right)^{-\frac{1}{\zeta_n(\{\mathbf{w}_k\}, \mathbf{S}) - 1}}. \quad (36)$$

Notice that function  $f(x) = x^{-\frac{1}{x-1}}$  increases monotonically for  $0 < x < 1$  and  $x > 1$ . Therefore, by letting  $\Gamma_d$  denote the solution to the equation  $f(x) = \Lambda$ , we equivalently rewrite the sensing eavesdropping constraints in (29c) as<sup>2</sup>

$$\frac{\beta_q(\{\mathbf{w}_k\}, \mathbf{S})}{\zeta_n(\{\mathbf{w}_k\}, \mathbf{S})} \leq \Gamma_d, \forall q \in \mathcal{Q}. \quad (37)$$

Finally, we reformulate the SINR constraints in (29a) as

$$\mathbf{h}_k^H \left( \mathbf{w}_k \mathbf{w}_k^H - \Gamma \left( \sum_{i \neq k} \mathbf{w}_i \mathbf{w}_i^H + \mathbf{S} \right) \right) \mathbf{h}_k \geq \Gamma \sigma^2, \forall k \in \mathcal{K}. \quad (38)$$

Similarly, we equivalently rewrite the information eavesdropping SNR constraints in (29b) as

$$\mathbf{g}_l^H \mathbf{w}_k \mathbf{w}_k^H \mathbf{g}_l \leq \Omega \sigma^2, \forall l \in \mathcal{L}, \forall k \in \mathcal{K}. \quad (39)$$

By combining (35), (37), (38), and (39), problem (P1) is equivalently reformulated as

$$\begin{aligned} \text{(P1.1)} : \quad & \min_{\{\mathbf{w}_k\}, \mathbf{S}} \quad \boldsymbol{\mu}^T (\boldsymbol{\Psi}^H \boldsymbol{\Psi})^{-1} \boldsymbol{\mu} \\ \text{s.t.} \quad & \text{(29d), (29e), (37), (38), and (39)}. \end{aligned}$$

It is noting that problem (P1.1) is still a non-convex problem due to the non-convexity of the objective function and the constraints in (37) and (38).

2) *SDR-Based Solution to Problem (P1.1)*: In the following, we present a SDR-based approach to address problem (P1.1). By introducing auxiliary variables  $\mathbf{W}_k = \mathbf{w}_k \mathbf{w}_k^H \succeq \mathbf{0}$  with  $\text{rank}(\mathbf{W}_k) \leq 1, \forall k \in \mathcal{K}$ , we equivalently reformulate the SINR constraints in (38) as

$$\mathbf{h}_k^H (\mathbf{W}_k - \Gamma \left( \sum_{i \neq k} \mathbf{W}_i + \mathbf{S} \right)) \mathbf{h}_k \geq \Gamma \sigma^2, \forall k \in \mathcal{K}. \quad (40)$$

Similarly, we equivalently reformulate (39) as

$$\mathbf{g}_l^H \mathbf{W}_k \mathbf{g}_l \leq \Omega \sigma^2, \forall l \in \mathcal{L}, \forall k \in \mathcal{K}. \quad (41)$$

Subsequently, we aim to address the sensing eavesdropping constraints in (37). Based on the expression of  $\beta_q(\{\mathbf{w}_k\}, \mathbf{S})$  and  $\zeta_n(\{\mathbf{w}_k\}, \mathbf{S})$  in Proposition 2, we equivalently reformulate (37) as

$$\mathbf{u}_q^H \mathbf{R} \mathbf{u}_q + N \sigma^2 \leq \Gamma_d \left( (\mathbf{a}_q + \mathbf{u}_q)^H \mathbf{R} (\mathbf{a}_q + \mathbf{u}_q) + N \sigma^2 \right), \forall q \in \mathcal{Q}. \quad (42)$$

<sup>2</sup>For the eavesdropping probability, a larger denominator  $\zeta_n(\{\mathbf{w}_k\}, \mathbf{S})$  at (37) contributes to a decrease in the sensing eavesdropping detection probability. This denominator  $\zeta_n(\{\mathbf{w}_k\}, \mathbf{S})$  characterizes the received clutter plus noise power at the sensing eavesdroppers. Fundamentally, this indicates an opportunity to exploit clutter information to jam the sensing eavesdroppers. Conversely, a smaller numerator  $\beta_q(\{\mathbf{w}_k\}, \mathbf{S})$  represents the ability to decrease the received power at the sensing receivers when a target exists. This intentional reduction in received power aims to prevent the sensing eavesdroppers from detecting the presence of a target.

Furthermore, the transmit power constraints at ISAC transmitters in (29d) are equivalently reformulated as

$$\text{tr} \left( \mathbf{A}_i \left( \sum_{k=1}^K \mathbf{W}_k + \mathbf{S} \right) \mathbf{A}_i^H \right) \leq P, \forall i \in \mathcal{M}_t. \quad (43)$$

Moreover, recall that  $\boldsymbol{\Psi}^H \boldsymbol{\Psi}$  is affine w.r.t.  $\mathbf{R} = \sum_{k=1}^K \mathbf{W}_k + \mathbf{S}$  and thus equivalently affine w.r.t.  $\{\mathbf{W}_k\}$  and  $\mathbf{S}$ . Consequently, we equivalently reformulate problem (P1.1) as

$$\begin{aligned} \text{(P1.2)} : \quad & \min_{\{\mathbf{W}_k\}, \mathbf{S}} \quad \boldsymbol{\mu}^T (\boldsymbol{\Psi}^H \boldsymbol{\Psi})^{-1} \boldsymbol{\mu} \\ \text{s.t.} \quad & \text{(40), (41), (42), (43), and (29e)} \\ & \mathbf{W}_k \succeq \mathbf{0}, \text{rank}(\mathbf{W}_k) \leq 1, \forall k \in \mathcal{K}. \end{aligned} \quad (44a)$$

Notice that problem (P1.2) is still non-convex due to the non-convex rank constraints in (44a). Then we drop the rank constraints in (44a) and obtain the SDR version of problem (P1.2) as

$$\begin{aligned} \text{(SDR-1.2)} : \quad & \min_{\{\mathbf{W}_k\}, \mathbf{S}} \quad \boldsymbol{\mu}^T (\boldsymbol{\Psi}^H \boldsymbol{\Psi})^{-1} \boldsymbol{\mu} \\ \text{s.t.} \quad & \text{(40), (41), (42), (43), and (29e)}. \end{aligned}$$

In this context, (40), (41), (42), (43), and (29e) are all affine constraints w.r.t.  $\{\mathbf{W}_k\}$  and  $\mathbf{S}$ . Also notice that the inverse of a semidefinite matrix is a strict convex function [43]. As a result, the objective function  $\boldsymbol{\mu}^T (\boldsymbol{\Psi}^H \boldsymbol{\Psi})^{-1} \boldsymbol{\mu}$  is a strict convex function w.r.t.  $\{\mathbf{W}_k\}$  and  $\mathbf{S}$ . Therefore, problem (SDR-1.2) is a convex optimization problem that is solvable via an off-the-shelf toolbox, such as CVX [44]. Let  $\{\mathbf{W}_k^*\}$  and  $\mathbf{S}^*$  denote the optimal solution to problem (SDR-1.2) and  $\mathbf{R}^* = \sum_{k=1}^K \mathbf{W}_k^* + \mathbf{S}^*$ .

3) *Tightness of SDR*: In general, the optimal solution  $\{\mathbf{W}_k^*\}$  and  $\mathbf{S}^*$  may not satisfy the rank constraints in (44a) and thus are not necessarily optimal to the original problem (P1.2). In the following, we rigorously show the tightness of SDR in the following.

**Proposition 3.** Based on the obtained solution  $\{\mathbf{W}_k^*\}$  and  $\mathbf{S}^*$ , we can always construct an alternative solution as

$$\mathbf{W}_k^{\text{opt}} = \frac{\mathbf{W}_k^* \mathbf{h}_k \mathbf{h}_k^H \mathbf{W}_k^*}{\mathbf{h}_k^H \mathbf{W}_k^* \mathbf{h}_k}, \forall k \in \mathcal{K}, \quad (45)$$

$$\mathbf{S}^{\text{opt}} = \mathbf{R}^* - \sum_{k=1}^K \mathbf{W}_k^{\text{opt}}, \quad (46)$$

with  $\text{rank}(\mathbf{W}_k^{\text{opt}}) = 1, \forall k \in \mathcal{K}$ . The constructed solution  $\{\mathbf{W}_k^{\text{opt}}\}$  and  $\mathbf{S}^{\text{opt}}$  achieves the same optimal objective function achieved by solution  $\{\mathbf{W}_k^*\}$  and  $\mathbf{S}^*$  while satisfying the rank constraints in (44a). Therefore, the solution of  $\{\mathbf{W}_k^{\text{opt}}\}$  and  $\mathbf{S}^{\text{opt}}$  is globally optimal to problem (P1.2).

*Proof.* Please refer to Appendix C.  $\square$

Based on Proposition 3, the optimal solution to the joint secure transmit beamforming problem (P1) is finally obtained.

## V. ALTERNATIVE SECURE ISAC DESIGNS

In this section, we propose two alternative transmit beamforming designs for secure ISAC. The first alternative design focuses on maximizing the sensing SNR rather than directly maximizing detection probability. The second design involves coordinated transmit beamforming in a multi-cell ISAC configuration rather than cell-free transmission.

### A. Sensing SNR Maximization

In this subsection, we consider the sensing SNR maximization problem in the secure cell-free ISAC scenario, which is a widely adopted intuitive design objective [27]. Following the discussion in [27], the sensing SNR is defined as the ratio of the sum power at all sensing receivers to the sum noise power. The received power from transmitter  $i \in M_t$  to the target direction is given as  $\mathbf{a}_t^H(\theta_i)\mathbf{A}_i\mathbf{R}\mathbf{A}_i^H\mathbf{a}_t(\theta_i)$ . Consequently, the received sensing SNR is given as

$$\gamma_S(\{\mathbf{w}_k\}, \mathbf{S}) = \frac{\sum_{i=1}^{M_t} \mathbf{a}_t^H(\theta_i)\mathbf{A}_i\mathbf{R}\mathbf{A}_i^H\mathbf{a}_t(\theta_i)}{M_t\sigma_s^2}, \quad (47)$$

where  $\mathbf{R} = \mathbb{E}(\mathbf{x}(t)\mathbf{x}^H(t))$  is transmit covariance of the  $M_t$  ISAC transmitters. Consequently, we formulate a sensing SNR maximization problem within our secure cell-free ISAC system as follows, by replacing the objective function in (P1) as the sensing SNR in (47).

$$(P2) : \begin{aligned} & \max_{\{\mathbf{w}_k\}, \mathbf{S}} \frac{\sum_{i=1}^{M_t} \mathbf{a}_t^H(\theta_i)\mathbf{A}_i\mathbf{R}\mathbf{A}_i^H\mathbf{a}_t(\theta_i)}{M_t\sigma_s^2} \\ & \text{s.t.} \quad (29a), (29b), (29c), (29d), \text{ and } (29e). \end{aligned}$$

Based on the similar problem reformulation and SDR technique for problem (P1), we equivalently reformulate problem (P2) as

$$(P2.1) : \begin{aligned} & \min_{\{\mathbf{W}_k\}, \mathbf{S}} \sum_{i=1}^{M_t} \mathbf{a}_t^H(\theta_i)\mathbf{A}_i\mathbf{R}\mathbf{A}_i^H\mathbf{a}_t(\theta_i) \\ & \text{s.t.} \quad (40), (41), (42), (43), \text{ and } (29e). \\ & \quad \mathbf{W}_k \succeq \mathbf{0}, \text{rank}(\mathbf{W}_k) \leq 1, \forall k \in \mathcal{K}. \quad (49a) \end{aligned}$$

Then, we directly drop the rank constraints in (49a) and obtain the SDR version of problem (P2.1) as

$$(SDR-2.1) : \begin{aligned} & \min_{\{\mathbf{W}_k\}, \mathbf{S}} \sum_{i=1}^{M_t} \mathbf{a}_t^H(\theta_i)\mathbf{A}_i\mathbf{R}\mathbf{A}_i^H\mathbf{a}_t(\theta_i) \\ & \text{s.t.} \quad (40), (41), (42), (43), \text{ and } (29e). \end{aligned}$$

Due to the fact that the objective function is affine w.r.t.  $\{\mathbf{W}_k\}$  and  $\mathbf{S}$ , problem (SDR-2.1) is a convex optimization problem that is solvable via an off-the-shelf toolbox, such as CVX [44]. It can be similarly verified that the construction in Proposition 3 is also applicable here to obtain an optimal solution to problem (P2.1). Thus, problem (P2.1) can also be optimally solved.

### B. Coordinated Transmit Beamforming Design

In this subsection, we propose another alternative design based on coordinated beamforming. In the coordinated beamforming scenario, each CU is served only by one ISAC transmitter and the signals from different ISAC transmitters are independent [22]. Let  $\mathcal{K}_i$  denote the set of CUs associated to ISAC transmitter  $i \in M_t$ . Equivalently, the transmit beamforming vector at ISAC transmitter  $i \in M_t$  for CU  $k \notin \mathcal{K}_i$  is forced to be  $\mathbf{0}$ , i.e.,

$$\hat{\mathbf{w}}_{i,k} = \mathbf{0}, \forall i \in M_t, k \notin \mathcal{K}_i. \quad (50)$$

Then, we exploit the binary auxiliary matrix  $\mathbf{A}_i$  to transform (50) as

$$\mathbf{A}_i\mathbf{w}_k = \mathbf{0}, \forall i \in M_t, k \notin \mathcal{K}_i. \quad (51)$$

As a result, the detection probability maximization problem for coordinated transmit beamforming in the secure multi-cell ISAC system is formulated as

$$(P3) : \begin{aligned} & \max_{\{\mathbf{w}_k\}, \mathbf{S}} \Upsilon_{\tilde{\chi}^2(\lambda(\{\mathbf{w}_k\}, \mathbf{S}))}(\Psi) \\ & \text{s.t.} \quad (51), (29b), (29c), (29d), \text{ and } (29e). \end{aligned}$$

In the following, we present the optimal solution to problem (P3). To begin with, we utilize the same problem reformulation and SDR technique as in Section IV for problem (P3). Based on the constraints in (51), the auxiliary variables  $\mathbf{W}_k \in \mathbb{C}^{NM_t \times NM_t}$  should maintain the structure

$$\mathbf{W}_k = \text{blkdiag}(\mathbf{0}, \dots, \underbrace{\hat{\mathbf{w}}_{i,k}\hat{\mathbf{w}}_{i,k}^H}_{\text{The } i\text{-th matrix}}, \dots, \mathbf{0}), k \in \mathcal{K}_i. \quad (53)$$

We introduce new auxiliary variables  $\hat{\mathbf{W}}_k \in \mathbb{C}^{N \times N}$  and formulate the structure in (53) as

$$\mathbf{W}_k = \mathbf{J}_i \otimes \hat{\mathbf{W}}_k, \forall k \in \mathcal{K}, \quad (54)$$

where  $\mathbf{J}_i = \text{diag}(0, \dots, \underbrace{1}_{\text{The } i\text{-th element}}, \dots, 0)$ ,  $k \in \mathcal{K}_i$ . As a result, problem (P3) is reformulated as

$$(P3.1) : \begin{aligned} & \min_{\{\mathbf{W}_{i,k}, \mathbf{W}_k\}, \mathbf{S}} \boldsymbol{\mu}^T(\Psi^H\Psi)^{-1}\boldsymbol{\mu} \\ & \text{s.t.} \quad (54), (40), (41), (42), (43), \text{ and } (29e) \\ & \quad \mathbf{W}_k \succeq \mathbf{0}, \text{rank}(\mathbf{W}_k) \leq 1, \forall k \in \mathcal{K}. \quad (55a) \end{aligned}$$

Then, we drop the rank constraints in (55a) to obtain the SDR version of problem (P3.1):

$$(SDR-3.1) : \begin{aligned} & \min_{\{\mathbf{W}_k\}, \mathbf{S}, \{\mathbf{W}_{i,k}\}} \boldsymbol{\mu}^T(\mathbf{Y}^H\mathbf{Y})^{-1}\boldsymbol{\mu} \\ & \text{s.t.} \quad (54), (40), (41), (42), (43), \text{ and } (29e). \end{aligned}$$

Problem (SDR-3.1) is a convex optimization problem that is solvable via CVX. Let  $\{\mathbf{W}_k^*\}$ ,  $\mathbf{S}^*$ , and  $\{\hat{\mathbf{W}}_k^*\}$  denote the obtained solution and  $\mathbf{R}^* = \sum_{k=1}^K \mathbf{W}_k^* + \mathbf{S}^*$ . In the following, we rigorously show the tightness of SDR.

**Proposition 4.** Based on the obtained solution  $\{\mathbf{W}_k^*\}$ ,  $\mathbf{S}^*$ , and  $\{\hat{\mathbf{W}}_k^*\}$ , we construct

$$\hat{\mathbf{W}}_k^{\text{opt}} = \frac{\hat{\mathbf{W}}_k^* \mathbf{h}_{i,k} \mathbf{h}_{i,k}^H \hat{\mathbf{W}}_k^*}{\mathbf{h}_{i,k}^H \hat{\mathbf{W}}_k^* \mathbf{h}_{i,k}}, \quad (56)$$

$$\bar{\mathbf{W}}_k^{\text{opt}} = \mathbf{J}_i \otimes \hat{\mathbf{W}}_k^{\text{opt}}, \quad (57)$$

$$\bar{\mathbf{S}}^{\text{opt}} = \mathbf{R}^* - \sum_{k=1}^K \bar{\mathbf{W}}_k^{\text{opt}}, \quad (58)$$

with  $\text{rank}(\hat{\mathbf{W}}_k^{\text{opt}}) \leq 1, \forall k \in \mathcal{K}$ . As a result, the constructed solution  $\{\bar{\mathbf{W}}_k^{\text{opt}}\}$  and  $\bar{\mathbf{S}}^{\text{opt}}$ , and  $\{\hat{\mathbf{W}}_k^{\text{opt}}\}$  achieves the same optimal objective function and satisfies the rank constraints in (44a), which is thus optimal to problem (P3).

*Proof.* This proposition can be similarly proved as for Proposition 3. Therefore, the details are omitted.  $\square$

*Remark 2.* It is crucial to highlight that the objective of maximizing the sensing SNR in a cell-free system is equivalent to maximizing the trace of our covariance matrix in (34). While this design prioritizes maximizing the transmitted power toward the target direction, it may overlook the significance of non-diagonal elements in  $\mathbf{R}_\Phi$ . Indeed, these non-diagonal elements represent the covariance of signals from different ISAC transmitters, indicating that the sensing SNR maximization design might not fully leverage the joint signal processing gain in the cell-free network to maximize the detection probability, and thus may lead to sub-optimal performance in general. Next, the coordinated beamforming neglects the importance of the covariance of signals from different ISAC transmitters by allowing the independent signal transmission at ISAC transmitters for achieving lower implementation complexity. This, however, may lead to sub-optimal performance as compared to the optimal cell-free architecture. The arguments will be validated in Section VI.

## VI. NUMERICAL RESULTS

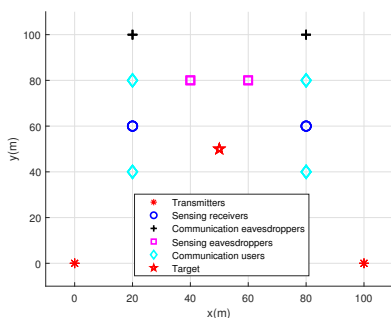


Fig. 2. Simulation topology of the secure cell-free ISAC system.

In this section, we provide numerical results to validate the performance of our proposed joint beamforming solution for the secure cell-free ISAC system. If not explicitly specified, the topology of our considered cell-free ISAC system is illustrated in Fig. 2. Within a  $100 \text{ m} \times 100 \text{ m}$  field, we position  $M_t = 2$  ISAC transmitters at  $[0 \text{ m}, 0 \text{ m}]$  and  $[100 \text{ m}, 0 \text{ m}]$ , and  $M_r = 2$

receivers at  $[20 \text{ m}, 60 \text{ m}]$  and  $[80 \text{ m}, 60 \text{ m}]$ , respectively. The target of interest is situated at  $[50 \text{ m}, 50 \text{ m}]$ . Additionally, there are  $K = 4$  CUs located at  $[20 \text{ m}, 40 \text{ m}]$ ,  $[20 \text{ m}, 80 \text{ m}]$ ,  $[80 \text{ m}, 40 \text{ m}]$ , and  $[80 \text{ m}, 80 \text{ m}]$ ,  $L = 2$  information eavesdroppers positioned at  $[20 \text{ m}, 100 \text{ m}]$  and  $[80 \text{ m}, 100 \text{ m}]$ , as well as  $Q = 2$  sensing eavesdroppers placed at  $[40 \text{ m}, 80 \text{ m}]$  and  $[60 \text{ m}, 80 \text{ m}]$ . The path-loss at a reference distance of 1 m is  $-40 \text{ dB}$ , while the path-loss exponent is standardized at 3. The noise power is set as  $\sigma^2 = \sigma_s^2 = -100 \text{ dBm}$ . The reflection coefficient w.r.t. RCS is a Gaussian random variable with zero mean and variance 0.01. The communication channel between each ISAC transmitter and the CUs or information eavesdroppers is modeled using Rician fading with a Rician factor of  $K_r = 5 \text{ dB}$ . The clutter channel of sensing eavesdroppers is generated by two randomly located scatterers in this area. Furthermore, the communication SINR threshold is established at  $\Gamma = 10 \text{ dB}$ , and the information eavesdropping SNR threshold is set as  $\Omega = 5 \text{ dB}$ . Moreover, the false alarm probability is standardized at 0.05, while the threshold for eavesdropping probability is set as  $\Lambda = 0.4$ .

For the purpose of comparison, we also illustrate an upper bound on the detection probability through a sensing only scheme, where only the transmit power constraints in problem (P1) are taken into account. This sensing only scheme serves as an upper limit in the cell-free ISAC system.

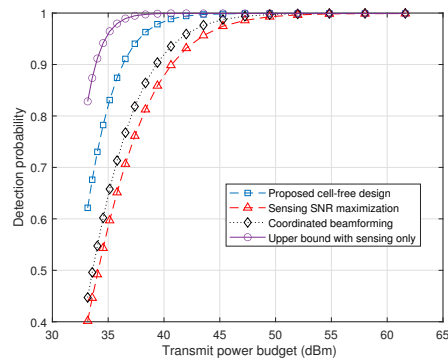


Fig. 3. The detection probability versus transmit power budget  $P$ .

Fig. 3 shows the detection probability versus the transmit power budget  $P$  at each transmitter. Notably, the sensing only scheme serves as a performance upper bound for maximizing the detection probability in this scenario. Furthermore, the two benchmark schemes exhibit similar performance and maintain a gap to our proposed design. This arises from the fact that the two benchmark schemes consider only the diagonal elements in the covariance matrix of  $\mathbf{R}_\Phi$  individually designing signals at each transmitter. In contrast, the proposed optimal solution, leveraging joint processing of sensing data in the central controller, can effectively exploit the covariance between different transmitters to maximize the detection probability.

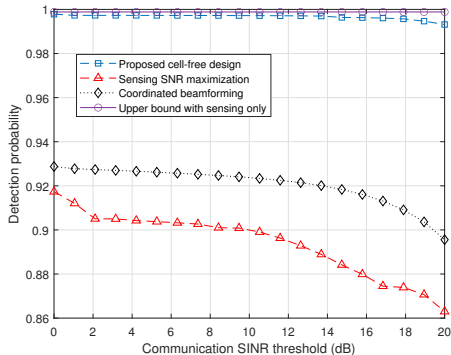


Fig. 4. The detection probability versus communication SINR threshold  $\Gamma$ .

Fig. 4 shows the detection probability versus the communication SINR threshold  $\Gamma$  with  $P = 43$  dBm. It is observed that the detection performance of all three methods decreases as  $\Gamma$  increases. This is due to the fact that as the SINR requirements become more stringent, more resource is allocated to communication to satisfy the need. Besides, our proposed design demonstrates its excellent robustness against the increase of communication SINR thresholds. In particular, the performance of the SNR maximization design experiences a rapid reduction with  $\Gamma$  increasing. In contrast, the proposed design and coordinated beamforming design are generally insensitive to the variation of  $\Gamma$ . This is because that the SNR maximization method is more sensitive to the spatial-domain energy distribution. A higher communication threshold directly leads to less energy at the target direction, and thus diminishes its performance.

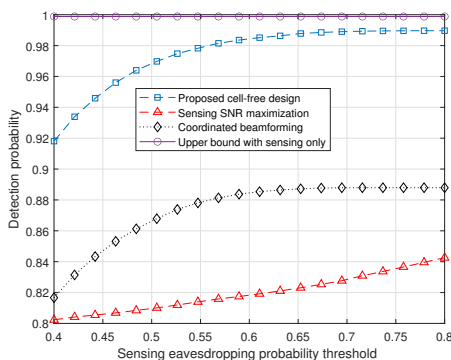


Fig. 5. The detection probability versus sensing eavesdropping probability threshold  $\Lambda$ .

Fig. 5 shows the detection probability versus the sensing eavesdropping probability threshold  $\Lambda$  with power budget  $P = 40$  dBm. It is evident that a more relaxed sensing eavesdropping probability constraint or a larger value of  $\Lambda$  results in a higher detection probability. Additionally, the proposed design consistently outperforms the coordinated beamforming design, and achieves a detection probability that is 10% higher than that by the sensing SNR maximization and the coordinated beamforming. This observation underscores the superiority of the cell-free architecture.

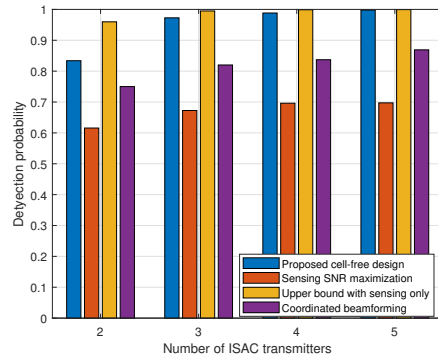


Fig. 6. The detection probability versus number of ISAC transmitters  $M_t$ .

Fig. 6 shows the detection probability versus the number of ISAC transmitters  $M_t$ , in which the ISAC transmitters are randomly located in the region, and the total transmit power is fixed with  $P = 43$  dBm/ $M_t$ . In this case, it is evident that the detection probability increases with the number of ISAC transmitters. This is attributed to the fact that more ISAC transmitters allow for information acquisition from different angles, providing a spatial diversity gain for the multi-static sensing, thereby improving the multi-static sensing performance.

## VII. CONCLUSION

This paper investigated the joint design of transmit beamforming for a secure cell-free ISAC system, where multiple ISAC transmitters collaboratively serve multiple CUs while concurrently performing target detection in a specified area. The scenario included the presence of multiple information eavesdroppers attempting to intercept confidential CU data and sensing eavesdroppers aiming to extract target information from received echo signals. We formulated a transmit beamforming optimization problem with the objective of maximizing the detection probability while satisfying the SINR constraints for CUs, SNR constraints for information eavesdroppers, sensing eavesdropping detection probability constraints for sensing eavesdroppers, and transmit power constraints for each transmitter. We obtained the global optimal solution using a SDR-based method, with a rigorous proof of the relaxation's tightness. Furthermore, we formulated two alternative designs based on sensing SNR maximization and coordinated beamforming. Numerical results validated the effectiveness of our proposed design, as compared with the two alternative designs.

There are several interesting extensions for future research in secure cell-free ISAC systems. First, this paper can be extended to other scenarios with practical constraints, such as imperfect channel state information (CSI) and time synchronization among ISAC transmitters. Furthermore, investigating the operation of distributed optimization in large-scale cell-free ISAC networks presents another direction for future exploration. These extensions hold the potential to enhance the understanding and performance of secure cell-free ISAC systems in diverse and expansive scenarios.

APPENDIX A  
PROOF OF PROPOSITION 1

For a given  $\alpha$ , the probability density function (pdf) of  $\mathbf{y}_s$  is given as

$$p(\mathbf{r}_S; \alpha) = \frac{1}{(\pi\sigma_s^2)^{NM,T}} \exp\left(-\frac{1}{\sigma_s^2}(\mathbf{r}_S - \Psi\alpha)^H(\mathbf{r}_S - \Psi\alpha)\right). \quad (59)$$

The GLRT detector is expressed as

$$L_G(\mathbf{r}_S) = \frac{p(\mathbf{r}_S; \hat{\alpha}_1)}{p(\mathbf{r}_S; \hat{\alpha}_0)} \stackrel{\geq}{\leq} \Gamma, \quad (60)$$

where  $\Gamma$  is a given decision threshold w.r.t. the false alarm probability, and  $\hat{\alpha}_1$  and  $\hat{\alpha}_0$  are the maximum likelihood estimation (MLE) for  $\alpha$  under conditions  $\mathcal{H}_1$  and  $\mathcal{H}_0$ , respectively. Specifically,  $\hat{\alpha}_1$  is an unconstrained MLE calculated as

$$\hat{\alpha}_1 = (\Psi^H \Psi)^{-1} \Psi^H \mathbf{r}_S. \quad (61)$$

On the other hand,  $\hat{\alpha}_0$  is a constrained MLE subject to the constraint  $\mu^T \hat{\alpha}_0 = 0$ , which can be derived via the Lagrange multiplier method [45]. The problem of calculating  $\hat{\alpha}_0$  is given as

$$\min_{\hat{\alpha}_0} \|\mathbf{r}_S - \Psi \hat{\alpha}_0\|^2 \quad \text{s.t.} \quad \mu^T \hat{\alpha}_0 = 0.$$

The Lagrangian is given as

$$L(\hat{\alpha}_0) = \|\mathbf{r}_S - \Psi \hat{\alpha}_0\|^2 + \rho \mu^T \hat{\alpha}_0, \quad (62)$$

where  $\rho$  represents the Lagrange multiplier for constraint  $\mu^T \hat{\alpha}_0 = 0$ . By checking the derivation of  $L(\hat{\alpha}_0)$ , we have

$$\frac{\partial L(\hat{\alpha}_0)}{\partial \hat{\alpha}_0} = -2\Psi^H \mathbf{r}_S + 2\Psi^H \Psi \hat{\alpha}_0 + \rho \mu. \quad (63)$$

By setting the derivative in (63) equal to  $\mathbf{0}$ , we have

$$\hat{\alpha}_0 = \underbrace{(\Psi^H \Psi)^{-1} \Psi^H \mathbf{r}_S}_{\hat{\alpha}_1} - (\Psi^H \Psi)^{-1} \frac{\rho \mu}{2}. \quad (64)$$

Then, we can easily calculate  $\rho \geq 0$  as

$$\begin{aligned} \mu^T \hat{\alpha}_0 &= 0 \\ \Rightarrow \mu^T [(\Psi^H \Psi)^{-1} \Psi^H \mathbf{r}_S - (\Psi^H \Psi)^{-1} \frac{\rho \mu}{2}] &= 0 \\ \Rightarrow \frac{\rho}{2} &= \frac{\mu^T (\Psi^H \Psi)^{-1} \Psi^H \mathbf{r}_S}{\mu^T (\Psi^H \Psi)^{-1} \mu} = \frac{\mu^T \hat{\alpha}_1}{\mu^T (\Psi^H \Psi)^{-1} \mu}. \end{aligned} \quad (65)$$

Consequently,  $\hat{\alpha}_0$  is given as

$$\hat{\alpha}_0 = \hat{\alpha}_1 - \frac{(\Psi^H \Psi)^{-1} \mu^T \hat{\alpha}_1 \mu}{\mu^T (\Psi^H \Psi)^{-1} \mu}. \quad (66)$$

As a result, the expression for  $\ln(L_G(\mathbf{y}_s))$  is

$$\begin{aligned} \ln(L_G(\mathbf{r}_S)) &= -\frac{1}{\sigma_s^2} [(\mathbf{r}_S - \Psi \hat{\alpha}_1)^H (\mathbf{r}_S - \Psi \hat{\alpha}_1) \\ &\quad - (\mathbf{r}_S - \Psi \hat{\alpha}_0)^H (\mathbf{r}_S - \Psi \hat{\alpha}_0)]. \end{aligned} \quad (67)$$

After some mathematical derivation, we have

$$\ln(L_G(\mathbf{r}_S)) = \frac{|\mu^T \hat{\alpha}_1|^2}{\sigma_s^2 \mu^T (\Psi^H \Psi)^{-1} \mu}. \quad (68)$$

Then we calculate the distribution of  $\ln(L_G(\mathbf{r}_S))$  under two different conditions. Notice that  $\hat{\alpha}_1 \sim \mathcal{CN}(\alpha, \sigma_s^2(\Psi^H \Psi)^{-1})$ , and accordingly we have

$$\mu^T \hat{\alpha}_1 \sim \begin{cases} \mathcal{CN}(\mathbf{0}, \sigma_s^2 \mu^T (\Psi^H \Psi)^{-1} \mu), & \mathcal{H}_0, \\ \mathcal{CN}(\mu^T \alpha, \sigma_s^2 \mu^T (\Psi^H \Psi)^{-1} \mu), & \mathcal{H}_1. \end{cases} \quad (69)$$

As a result, the distribution of  $\ln(L_G(\mathbf{r}_S))$  is given as

$$\ln(L_G(\mathbf{y}_s)) \sim \begin{cases} \chi^2, & \mathcal{H}_0, \\ \tilde{\chi}^2(\lambda), & \mathcal{H}_1, \end{cases} \quad (70)$$

where  $\lambda = \frac{|\mu^T \alpha|^2}{\sigma_s^2 \mu^T (\Psi^H \Psi)^{-1} \mu}$ . This completes the proof.

APPENDIX B  
PROOF OF PROPOSITION 2

Based on the Neyman-Pearson criterion, the optimal detection rule for the sensing eavesdropper is given as

$$L_G(\tilde{r}_q(t)) = \frac{p_0(\tilde{r}_q(t))}{p_1(\tilde{r}_q(t))} \stackrel{\geq}{\leq} 1, \quad (71)$$

which can be expressed as

$$|\tilde{r}_q(t)|^2 \stackrel{\geq}{\leq} \frac{\zeta_q(\{\mathbf{w}_k\}, \mathbf{S}) \beta_q(\{\mathbf{w}_k\}, \mathbf{S})}{\beta_q(\{\mathbf{w}_k\}, \mathbf{S}) - \zeta_q(\{\mathbf{w}_k\}, \mathbf{S})} \ln\left(\frac{\beta_q(\{\mathbf{w}_k\}, \mathbf{S})}{\zeta_q(\{\mathbf{w}_k\}, \mathbf{S})}\right). \quad (72)$$

According to (25), the cumulative density functions (CDFs) under  $\tilde{\mathcal{H}}_0$  and  $\tilde{\mathcal{H}}_1$  are respectively given as

$$\Pr(|\tilde{r}_q(t)|^2 | \tilde{\mathcal{H}}_0) = 1 - \exp\left(-\frac{|\tilde{r}_q(t)|^2}{\zeta_q(\{\mathbf{w}_k\}, \mathbf{S})}\right), \quad (73)$$

$$\Pr(|\tilde{r}_q(t)|^2 | \tilde{\mathcal{H}}_1) = 1 - \exp\left(-\frac{|\tilde{r}_q(t)|^2}{\beta_q(\{\mathbf{w}_k\}, \mathbf{S})}\right). \quad (74)$$

By substituting (72) into (74), we obtain

$$\tilde{p}_q(\{\mathbf{w}_k\}, \mathbf{S}) = \left(\frac{\beta_q(\{\mathbf{w}_k\}, \mathbf{S})}{\zeta_q(\{\mathbf{w}_k\}, \mathbf{S})}\right)^{-\frac{\zeta_q(\{\mathbf{w}_k\}, \mathbf{S})}{\beta_q(\{\mathbf{w}_k\}, \mathbf{S}) - \zeta_q(\{\mathbf{w}_k\}, \mathbf{S})}}. \quad (75)$$

This completes the proof.

APPENDIX C  
PROOF OF PROPOSITION 3

First, we consider the optimal objective function value. The optimal covariance matrix is given as

$$\mathbf{R}_x^* = \sum_{k=1}^K \mathbf{W}_k^{\text{opt}} + \mathbf{S}^{\text{opt}} = \sum_{k=1}^K \mathbf{W}_k^* + \mathbf{S}^*. \quad (76)$$

This implies that the objective function values achieved by  $\{\mathbf{W}_k^{\text{opt}}\}$  and  $\mathbf{S}^{\text{opt}}$  are equivalent to that of  $\{\mathbf{W}_k^*\}$  and  $\mathbf{S}^*$ . Furthermore, the constraints specified in (37) and (44a) are satisfied. Subsequently, by observing that the SINR constraints in (38) are satisfied due to the equality  $\mathbf{h}_k^H \mathbf{W}_k^* \mathbf{h}_k = \mathbf{h}_k^H \mathbf{W}_k^{\text{opt}} \mathbf{h}_k$ ,  $\forall k \in \mathcal{K}$ . Then, by letting  $\mathbf{v} \in \mathbb{C}^{NM_t \times 1}$  denote an arbitrary vector, we have

$$\mathbf{v}^H (\mathbf{W}_k^* - \mathbf{W}_k^{\text{opt}}) \mathbf{v} = \mathbf{v}^H \mathbf{W}_k^* \mathbf{v} - \frac{|\mathbf{v}^H \mathbf{W}_k^* \mathbf{h}_k|^2}{\mathbf{h}_k^H \mathbf{W}_k^* \mathbf{h}_k}. \quad (77)$$

Based on the Cauchy-Schwarz inequality [17], we have  $(\mathbf{v}^H \mathbf{W}_k^* \mathbf{v})(\mathbf{h}_k^H \mathbf{W}_k^* \mathbf{h}_k) \geq |\mathbf{v}^H \mathbf{W}_k^* \mathbf{h}_k|^2$ . As a result,  $\mathbf{W}_k^* - \mathbf{W}_k^{\text{opt}} \succeq \mathbf{0}$ ,  $\forall k \in \mathcal{K}$ . Consequently, we have

$$\mathbf{g}_l^H \mathbf{W}_k^{\text{opt}} \mathbf{g}_l \leq \mathbf{g}_l^H \mathbf{W}_k^* \mathbf{g}_l \leq \Lambda \sigma^2, \forall l \in \mathcal{L}. \quad (78)$$

Hence, the constraints in (39) are also satisfied. This completes the proof.

## REFERENCES

- [1] ITU-R, "Framework and Overall Objectives of the Future Development of IMT for 2030 and Beyond," International Telecommunication Union - Radiocommunication Sector (ITU-R), Internal Document, September 2023. [Online]. Available: <https://www.itu.int/en/ITU-R/study-groups/rsg5/rwp5d/imt-2030/Pages/default.aspx>
- [2] L. U. Khan, W. Saad, D. Niyato, Z. Han, and C. S. Hong, "Digital-twin-enabled 6G: Vision, architectural trends, and future directions," *IEEE Commun. Mag.*, vol. 60, no. 1, pp. 74–80, 2nd quarter 2022.
- [3] L. Li, X. Zeng, Y.-F. Liu, Y. Xu, and T.-H. Chang, "CSI sensing from heterogeneous user feedbacks: A constrained phase retrieval approach," *IEEE Trans. Wireless Commun.*, vol. 22, no. 10, pp. 6930–6945, Feb. 2023.
- [4] F. Liu, Y. Cui, C. Masouros, J. Xu, T. X. Han, Y. C. Eldar, and S. Buzzi, "Integrated sensing and communications: Towards dual-functional wireless networks for 6G and beyond," *IEEE J. Sel. Areas Commun.*, vol. 40, no. 6, pp. 1728–1767, Jun. 2022.
- [5] F. Liu, L. Zheng, Y. Cui, C. Masouros, A. P. Petropulu, H. Griffiths, and Y. C. Eldar, "Seventy years of radar and communications: The road from separation to integration," *IEEE Signal Process. Mag.*, vol. 40, no. 5, pp. 106–121, Jul. 2023.
- [6] C. Masouros, R. W. Heath, J. A. Zhang, Z. Feng, L. Zheng, and A. P. Petropulu, "Introduction to the issue on joint communication and radar sensing for emerging applications," *IEEE J. Sel. Topics Signal Process.*, vol. 15, no. 6, pp. 1290–1294, Dec. 2021.
- [7] Y. Xiong, F. Liu, Y. Cui, W. Yuan, T. X. Han, and G. Caire, "On the fundamental tradeoff of integrated sensing and communications under Gaussian channels," *IEEE Trans. Inf. Theory*, vol. 69, no. 9, pp. 5723–5751, Jun. 2023.
- [8] H. Hua, T. X. Han, and J. Xu, "MIMO integrated sensing and communication: CRB-rate tradeoff," *IEEE Trans. Wireless Commun.*, early access, Aug. 2022, doi: 10.1109/TWC.2023.3303326.
- [9] C. Ouyang, Y. Liu, H. Yang, and N. Al-Dhahir, "Integrated sensing and communications: A mutual information-based framework," *IEEE Commun. Mag.*, vol. 61, no. 5, pp. 26–32, May. 2023.
- [10] Z. Xiao and Y. Zeng, "Waveform design and performance analysis for full-duplex integrated sensing and communication," *IEEE J. Sel. Areas Commun.*, vol. 40, no. 6, pp. 1823–1837, Mar. 2022.
- [11] X. Liu, T. Huang, N. Shlezinger, Y. Liu, J. Zhou, and Y. C. Eldar, "Joint transmit beamforming for multiuser MIMO communications and MIMO radar," *IEEE Trans. Signal Process.*, vol. 68, pp. 3929–3944, Jun. 2020.
- [12] F. Liu, Y.-F. Liu, A. Li, C. Masouros, and Y. C. Eldar, "Cramér-Rao bound optimization for joint radar-communication beamforming," *IEEE Trans. Signal Process.*, vol. 70, pp. 240–253, Dec. 2022.
- [13] F. Sohrabi, T. Jiang, W. Cui, and W. Yu, "Active sensing for communications by learning," *IEEE J. Sel. Areas Commun.*, vol. 40, no. 6, pp. 1780–1794, Mar. 2022.
- [14] M. L. Rahman, J. A. Zhang, X. Huang, Y. J. Guo, and R. W. Heath, "Framework for a perceptive mobile network using joint communication and radar sensing," *IEEE Trans. Aerosp. Electron. Syst.*, vol. 56, no. 3, pp. 1926–1941, Jun. 2020.
- [15] F. Liu, C. Masouros, A. Li, H. Sun, and L. Hanzo, "MU-MIMO communications with MIMO radar: From co-existence to joint transmission," *IEEE Trans. Wireless Commun.*, vol. 17, no. 4, pp. 2755–2770, Apr. 2018.
- [16] Z. Liu, S. Aditya, H. Li, and B. Clerckx, "Joint transmit and receive beamforming design in full-duplex integrated sensing and communications," *IEEE J. Sel. Areas Commun.*, vol. 41, no. 9, pp. 2907–2919, Jun. 2023.
- [17] Z. Wang, J. Wu, Y.-F. Liu, and F. Liu, "Globally optimal beamforming design for integrated sensing and communication systems," *arXiv preprint arXiv:2309.06674*, 2023.
- [18] D. Gesbert, S. Hanly, H. Huang, S. S. Shitz, O. Simeone, and W. Yu, "Multi-cell MIMO cooperative networks: A new look at interference," *IEEE J. Sel. Areas Commun.*, vol. 28, no. 9, pp. 1380–1408, Dec. 2010.
- [19] J. Wu, Z. Zhang, Y. Hong, and Y. Wen, "Cloud radio access network (C-RAN): a primer," *IEEE netw.*, vol. 29, no. 1, pp. 35–41, Jan. 2015.
- [20] E. Björnson and L. Sanguinetti, "Scalable cell-free massive MIMO systems," *IEEE Trans. Commun.*, vol. 68, no. 7, pp. 4247–4261, Apr. 2020.
- [21] D. Xu, C. Liu, S. Song, and D. W. K. Ng, "Integrated sensing and communication in coordinated cellular networks," *arXiv preprint arXiv:2305.01213*, 2023.
- [22] G. Cheng, Y. Fang, J. Xu, and D. W. K. Ng, "Optimal coordinated transmit beamforming for networked integrated sensing and communications," *arXiv preprint arXiv:2307.05127*, 2023.
- [23] Y. Huang, Y. Fang, X. Li, and J. Xu, "Coordinated power control for network integrated sensing and communication," *IEEE Trans. Veh. Technol.*, vol. 71, no. 12, pp. 13361–13365, Jul. 2022.
- [24] L. Liu, S. Zhang, R. Du, T. X. Han, and S. Cui, "Networked sensing in 6G cellular networks: Opportunities and challenges," *arXiv preprint arXiv:2206.00493*, 2022.
- [25] S. Elhoushy, M. Ibrahim, and W. Hamouda, "Cell-Free massive MIMO: A survey," *IEEE Commun. Surveys Tuts.*, vol. 24, no. 1, pp. 492–523, 1st quarter 2022.
- [26] Y. Cao and Q.-Y. Yu, "Joint resource allocation for user-centric cell-free integrated sensing and communication systems," *IEEE Commun. Lett.*, vol. 27, no. 9, pp. 2338–2342, Sep. 2023.
- [27] U. Demirhan and A. Alkhateeb, "Cell-free ISAC MIMO systems: Joint sensing and communication beamforming," *arXiv preprint arXiv:2301.11328*, 2023.
- [28] Z. Behdad, Ö. T. Demir, K. W. Sung, E. Björnson, and C. Cavadar, "Multi-static target detection and power allocation for integrated sensing and communication in cell-free massive MIMO," *arXiv preprint arXiv:2305.12523*, 2023.
- [29] F. Zeng, J. Yu, J. Li, F. Liu, D. Wang, and X. You, "Integrated sensing and communication for network-assisted full-duplex cell-free distributed massive mimo systems," *arXiv preprint arXiv:2311.05101*, 2023.
- [30] Z. Wei, F. Liu, C. Masouros, N. Su, and A. P. Petropulu, "Toward multifunctional 6G wireless networks: Integrating sensing, communication, and security," *IEEE Commun. Mag.*, vol. 60, no. 4, pp. 65–71, Apr. 2022.
- [31] N. Su, F. Liu, and C. Masouros, "Secure radar-communication systems with malicious targets: Integrating radar, communications, and jamming functionalities," *IEEE Trans. Wireless Commun.*, vol. 20, no. 1, pp. 83–95, Jan. 2021.
- [32] D. Xu, X. Yu, D. W. K. Ng, A. Schmeink, and R. Schober, "Robust and secure resource allocation for ISAC systems: A novel optimization framework for variable-length snapshots," *IEEE Trans. Commun.*, vol. 70, no. 12, pp. 8196–8214, Dec. 2022.
- [33] Z. Ren, L. Qiu, J. Xu, and D. W. K. Ng, "Robust transmit beamforming for secure integrated sensing and communication," *IEEE Trans. Commun.*, vol. 71, no. 9, pp. 5549–5564, Sep. 2023.
- [34] A. Dimas, M. A. Clark, B. Li, K. Psounis, and A. P. Petropulu, "On radar privacy in shared spectrum scenarios," in *IEEE Int. Conf. Acoust., Speech Signal Process. (ICASSP)*, 2019, pp. 7790–7794.
- [35] I. W. da Silva, D. P. Osorio, and M. Juntti, "Multi-static ISAC in cell-free massive MIMO: Precoder design and privacy assessment," *arXiv preprint arXiv:2309.13368*, 2023.
- [36] —, "Privacy performance of MIMO dual-functional radar-communications with internal adversary," *arXiv preprint arXiv:2302.06253*, 2023.
- [37] Z.-Q. Luo, W.-K. Ma, A. M.-C. So, Y. Ye, and S. Zhang, "Semidefinite relaxation of quadratic optimization problems," *IEEE Signal Process. Mag.*, vol. 27, no. 3, pp. 20–34, Apr. 2010.
- [38] H. Hua, J. Xu, and T. X. Han, "Optimal transmit beamforming for integrated sensing and communication," *IEEE Trans. Veh. Technol.*, vol. 72, no. 8, pp. 10588–10603, Mar. 2023.
- [39] X. Chen, R. Jia, and D. W. K. Ng, "On the design of massive non-orthogonal multiple access with imperfect successive interference cancellation," *IEEE Trans. Commun.*, vol. 67, no. 3, pp. 2539–2551, Nov. 2018.
- [40] D. E. Hack, L. K. Patton, B. Himed, and M. A. Saville, "Detection in passive MIMO radar networks," *IEEE Trans. Signal Process.*, vol. 62, no. 11, pp. 2999–3012, Apr. 2014.
- [41] S. M. Kay, *Fundamentals of Statistical Signal Processing, Volume 2: Detection Theory*. Pearson Education India, 2009.
- [42] X. Wang, Z. Fei, P. Liu, J. A. Zhang, Q. Wu, and N. Wu, "Sensing aided covert communications: Turning interference into allies," *arXiv preprint arXiv:2307.11345*, 2023.
- [43] R. A. Horn and C. R. Johnson, *Matrix Analysis*. Cambridge university press, 2012.
- [44] M. Grant and S. Boyd, "CVX: Matlab software for disciplined convex programming, version 2.1," 2014.
- [45] S. M. Kay, *Fundamentals of Statistical Signal Processing: Estimation Theory*. Prentice-Hall, Inc., 1993.